Improved photocatalytic activity of $La_2Ti_2O_7$ on azophloxine degradation: the effects of PEG2000

LILI YANG, ZHENG MA, WENJIE ZHANG*
School of Environmental and Chemical Engineering, Shenyang Ligong University, Shenyang 110159, China

Porous lanthanum titanate was synthesized through a sol-gel route using PEG2000. The addition of PEG2000 inhibits perovskite $La_2Ti_2O_7$ crystal growth, and crystallite size of $La_2Ti_2O_7$ decreases with increasing PEG2000. BET surface area of the samples increases from 15.3 m^2/g of the nonporous sample to 52.4 m^2/g of the sample obtained with 3 g of PEG2000. FT-IR and FT-Far IR spectra of $La_2T_2O_7$ samples show the effects of PEG2000 on the functional groups in the materials. The reaction rate constant is 0.0032 min^{-1} for the $La_2Ti_2O_7$ sample prepared without PEG2000, while the reaction rate constants are promoted to 0.0135 and 0.0191 min^{-1} when 1 and 3 g of PEG2000 are used to prepare the porous $La_2Ti_2O_7$. The enhanced photocatalytic activity of the porous $La_2Ti_2O_7$ can be attributed to the increasing porosity and decreasing crystallite size.

(Received November 11, 2018; accepted August 20, 2019)

Keywords: Lanthanum titanate, Photocatalytic, Azophloxine, Degradation, PEG2000

1. Introduction

Organic hazardous substances in the industrial wastewater have to be removed before discharging into the aquatic system. However, wastewater containing some hazardous organic pollutants cannot be purified through the traditional bio-chemical process, since microorganisms cannot survive in such kinds of wastewater. As one of the advanced oxidation techniques, photocatalysis has been studied for deep oxidation of many organic substances to reduce the potential threaten to the environment [1-6]. Organic pollutants such as industrial dyes can be decomposed during photocatalytic oxidation process [7,8].

Photocatalytic oxidation efficiency depends on the activity of photocatalyst, and some kinds of materials have been developed besides the mostly applied titania [9-11]. For example, titanate in perovskite or pyrochloro structure has aroused great attention [12-16]. Strontium titanate and barium titanate were applied to both water splitting and water treatment [17-19]. Perovskite-type $La_2Ti_2O_7$ was reported to decompose bisphenol A and dye in the wastewater [20,21]. High temperature thermal treatment is usually necessary in the preparation of titanates, which can result in particles aggregation and weak activity of the material. Porous structure of materials can be modified by the addition of pore forming reagent during synthesizing route. Polyethylene glycol (PEG) was used to prepare TiO_2-$InVO_4$ nanoparticles for improved activity on methylene degradation [22]. Meanwhile, the application of PEG4000 template on synthesis of porous cerium titanate was reported in our previous work [15].

Porous lanthanum titanate was synthesized through a sol-gel route with the help of PEG2000 in this work. The materials were characterized using X-ray powder diffraction (XRD), transmission electron microscopy (TEM), surface area and pore analysis, and Fourier transform infrared/far infrared spectroscopy (FT-IR/FIR). Photocatalytic degradation of azophloxine on the lanthanum titanate materials was examined to clarify the effects of PEG2000.

2. Experimental methods

2.1. Preparation of porous lanthanum titanate

A traditional sol-gel method was used to prepare porous lanthanum titanate. The first solution was made from 8 mL ethanol and 0.85 mL tetrabutyl titanate, and the second solution was made from 1.0825 g lanthanum nitrate, 8 mL deionized water, 2 mL ethylene glycol, 8 mL acetic acid and different amount of PEG2000. The two solutions were mixed to prepare the transparent sol, followed by sol-gel transformation at 70 ^oC. The gel was dehydrated at 110 ^oC for 12 h, and then the solid was calcined at 800 ^oC for 3 h. The product was ground into fine powders before use.

2.2. Characterization methods

X-ray diffraction patterns of the samples were determined on D8 X-ray diffractometer using Cu *K*α radiation. TEM images of the materials were taken on FEI Tecnai G2 20 transmittance electron microscope. Specific surface area and porous structure measurements were performed on ASAP 2460 surface area and pore size

analyzer. Specific surface area was determined by the multipoint Brunauer-Emmett-Teller (BET) method [23], and pore volume distribution was determined using the Barrett-Joyner-Halenda (BJH) method [24]. Infrared and far infrared absorption spectra were determined by Frontier FT-IR/FIR spectrometer.

2.3. Photocatalytic activity measurement

The reactor for photocatalytic activity determination was made of a 100 mL quartz beaker and a 20 W UV lamp. 30 mg $La_2Ti_2O_7$ was mixed with 50 mL of 40 mg/L azophloxine solution, and the mixture was stirred in the dark for 30 min to reach adsorption-desorption equilibrium. Photocatalytic oxidation of azophloxine was triggered by 2300 $\mu W/cm^2$ of UV irradiation at wavelength of 253.7 nm. After removing the solid photocatalyst from the azophloxine solution, the concentration of azophloxine solution was determined by 721E spectrophotometer at the maximum absorption wavelength of 506 nm. UV-Vis spectra of azophloxine solution were recorded by LAMBDA 35 UV-Vis spectrometer.

3. Results and discussion

3.1. Characterization of porous lanthanum titanate

X-ray diffraction patterns of the $La_2Ti_2O_7$ samples obtained with different amount of PEG2000 are presented in Fig. 1. The diffraction patterns are attributed to perovskite $La_2Ti_2O_7$ in monoclinic system, which are in accordance to the pattern in JCPDS 81-1066. Impurities of other phases of lanthanum titanate are not found in the patterns, while the diffraction intensity is reduced after the addition of PEG2000 [25]. Obviously, the existence of PEG2000 in the precursor can put effect on crystallization of perovskite $La_2Ti_2O_7$. The diffraction peak at 2θ=29.8 corresponds to the preferred (-212) plane, and Scherrer formula was used to calculate the crystallite size at this plane [26]. The crystallite sizes are 38.5, 33.8, 28.6 and 27.5 nm for the $La_2Ti_2O_7$ samples obtained using 0, 1, 3 and 5 g of PEG2000. The addition of PEG2000 inhibits perovskite $La_2Ti_2O_7$ crystal growth, leading to decreasing crystallite size. The macromolecular polyethylene glycol is surrounded by tetrabutyl titanate molecules to form a complex in the precursor, so that the subsequent hydrolysis of tetrabutyl titanate occurs on the complex. Extensive dehydration of Ti-OH groups is difficult in such circumstance to prevent the formation of huge three-dimensional Ti-O-Ti network. Consequently, crystallization of perovskite $La_2Ti_2O_7$ may occur on more nucleation centers during calcination [27].

Fig. 2 gives the TEM images of $La_2Ti_2O_7$ samples obtained without PEG2000 and using 3 g of PEG2000. The crystals in the nonporous sample aggregate into large particle, in which the crystals may fuse into each other. There is no apparent porous structure in the large particles. On the other hand, inter-crystal holes can be identified in the porous sample. The crystallite size is almost the same to the value calculated from X-ray diffraction peak. Polyethylene glycol molecules are removed during calcination, leaving holes in the porous material, although the crystals may also fuse into each other during calcination.

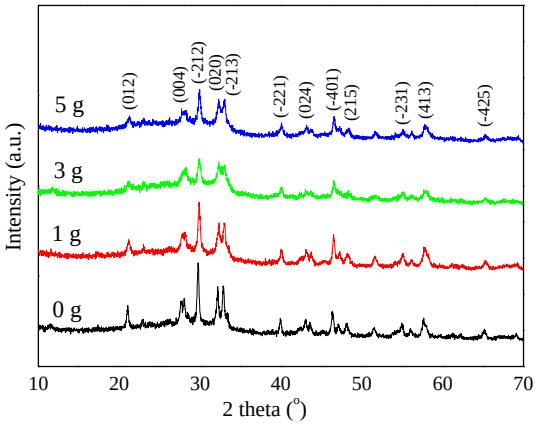

Fig. 1. XRD patterns of $La_2Ti_2O_7$ samples obtained using different amount of PEG2000 in the precursor

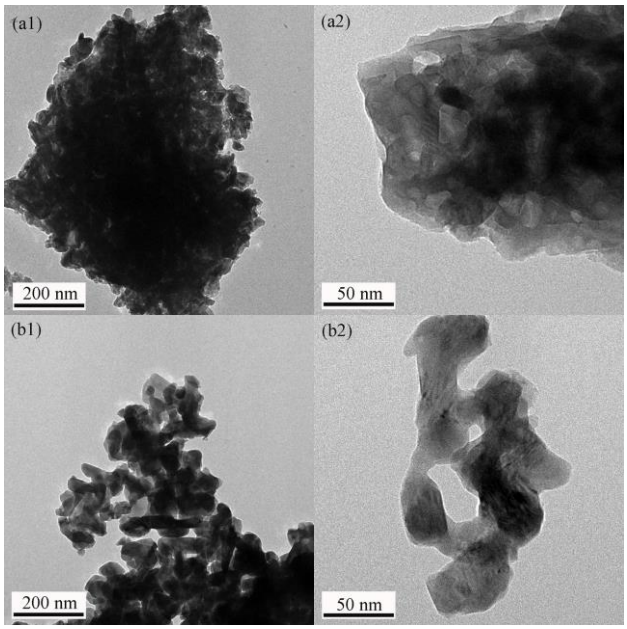

Fig. 2. TEM images of $La_2Ti_2O_7$ samples. (a) Obtained without PEG2000, (b) Obtained using 3 g of PEG2000

Fig. 3a illustrates N_2 adsorption-desorption isotherms of the $La_2Ti_2O_7$ samples as a factor of PEG2000 amount. The amount of N_2 molecules adsorbed on the materials smoothly increases with rising N_2 relative pressure, indicating the monolayer or multilayer adsorption of N_2 molecules on the materials. The abrupt increase of adsorbed N_2 molecules when P/P_0 is more than 0.9 is due to capillary condensation of N_2 molecules in the macropores. According to the shape of hysteretic loop in the high pressure region of the isotherms, all the adsorption-desorption isotherms can be classified as

IUPAC type IV, showing mesoporous character of the samples. The H3 type hysteretic loop is related to porous material with broad pore size distribution.

Fig. 3b presents the pore size distribution in the $La_2Ti_2O_7$ samples with respect to PEG2000 amount. BET surface area, average pore size and total pore volume of the $La_2Ti_2O_7$ samples were calculated from the pore size distribution curves. The average pore size of the nonporous sample is 15.5 nm, while the average pore sizes the samples obtained using 3 and 5 g of PEG2000 are round 30 nm. Both the BET surface area and total pore volume of the samples are enlarged after using PEG2000. BET surface area of the samples increases from 15.3 m^2/g of the nonporous sample to 52.4 m^2/g of the sample obtained with 3 g of PEG2000. The total pore volume also increases from 0.06343 cm^3/g to 0.10762 cm^3/g at the same time. However, on the contrary, both the specific surface area and pore volume decrease in the sample obtained with 5 g of PEG2000. The removal of PEG2000 during calcination leaves mesopores in the materials, while the pores might collapse when excessive PEG2000 is used.

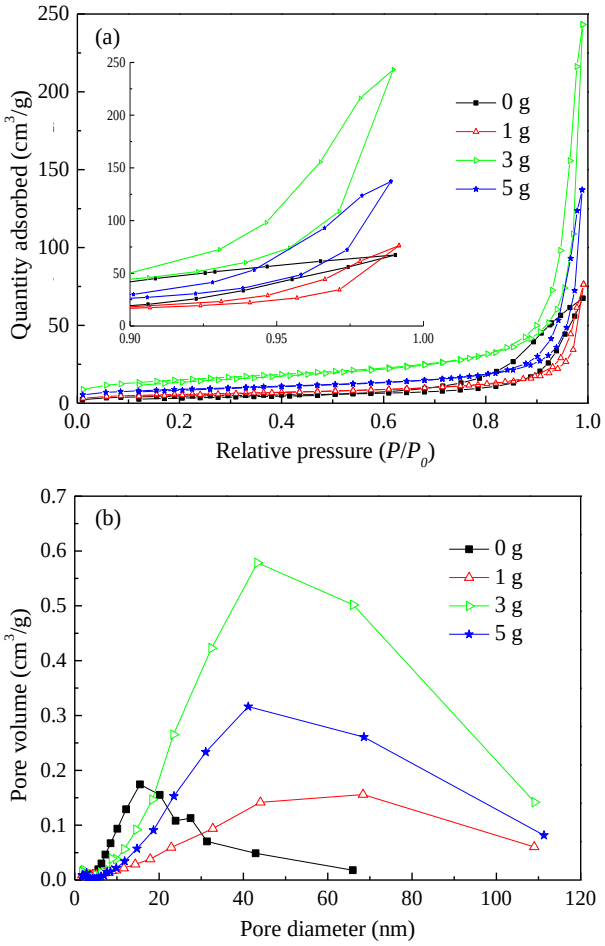

Fig. 3. (a) N_2 adsorption-desorption isotherms of $La_2Ti_2O_7$ samples, and (b) Pore size distribution in $La_2Ti_2O_7$ samples as a factor of PEG2000 amount

Fig. 4 shows FT-IR and FT-Far IR spectra of $La_2T_2O_7$ samples to clarify the effects of PEG2000 on the functional groups in the materials. As can be seen in Fig. 4a, the absorption peaks at 1634 and 3466 cm^{-1} are due to the vibration of hydroxyl group, which is mainly attributed to the adsorbed water on the materials [25]. The absorption intensity of hydroxyl group increases with rising PEG2000 amount, since more water molecules can be adsorbed on the surface of the porous materials. The absorptions at 2926 and 2855 cm^{-1} come from the asymmetric stretching vibration of methylene group, and the absorption at 1401 cm^{-1} is due to the bending vibration of methylene group [28]. The methylene groups belong to the organic residues that were not burnt out during calcination.

Ti-O bending vibration in octahedral TiO_6 has an absorption at 779 cm^{-1}, as shown in Fig. 4a, while absorptions of metal-oxides in the materials can be much easily identified in the FT-Far IR spectra in Fig. 4b. The bending vibration of Ti-O-La at 463 cm^{-1} and the absorptions of La-O stretching vibration at 348, 551 and 643 cm^{-1} are the characteristic absorptions of $La_2Ti_2O_7$ [21]. The absorption intensities of these bondings in the materials decrease after adding more PEG2000, showing the reduced crystallization of perovskite $La_2Ti_2O_7$. This is in accordance to the XRD results.

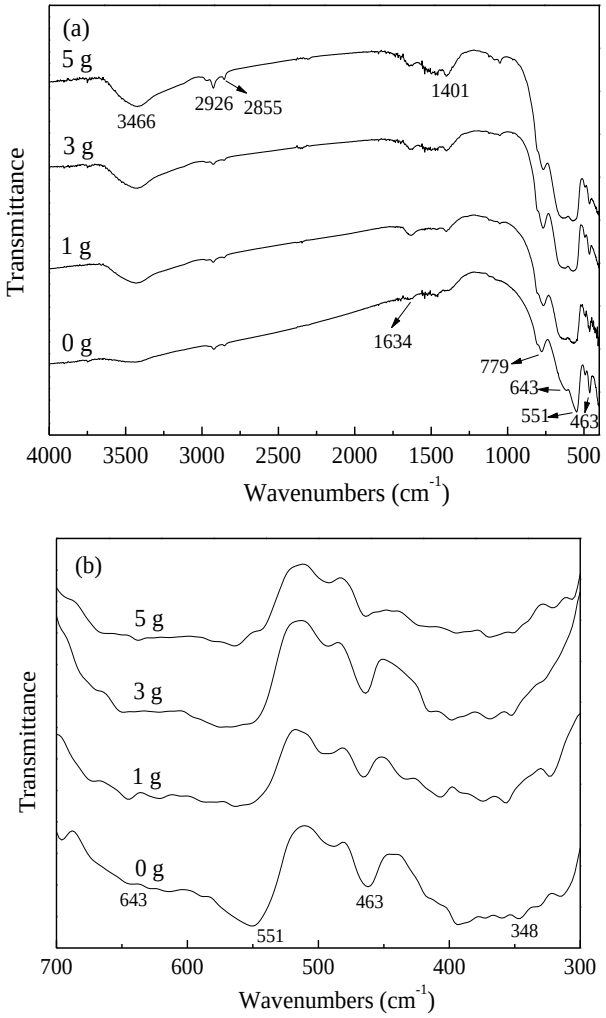

Fig. 4. (a) FT-IR and (b) FT-Far IR spectra of $La_2T_2O_7$ samples with respect to PEG2000 amount

3.2. Photocatalytic activity

The removal of azophloxine from water depends on both adsorption and photocatalytic degradation. Fig. 5 shows the removal efficiencies through adsorption and photocatalytic degradation of azophloxine on $La_2Ti_2O_7$ as a factor of PEG2000 amount. After adsorption-desorption equilibrium of azophloxine on the materials, photocatalytic degradation is initiated right after turning on the UV source. The adsorption efficiency does not noticeably change with the variation of PEG2000 amount, and the maximum adsorption percent is not more than 2.5%.

Photocatalytic degradation of azophloxine is responsible for the purification of the solution. The amount of PEG2000 has obvious effect on the degradation efficiency. The degradation efficiency is increased almost linearly with rising PEG2000 amount and reaches the maximum value for the sample using 3 g of PEG2000. After 30 min of irradiation, photocatalytic degradation efficiency is 32.6% on the optimal sample. The enhanced photocatalytic activity of the porous $La_2Ti_2O_7$ can be attributed to the increasing porous structure and decreasing crystallite size. It is accepted that small crystals usually have high activity. Since photocatalytic reaction occurs on the surface of the material, the enlarged surface area can inevitably add positive effects to degradation of azophloxine.

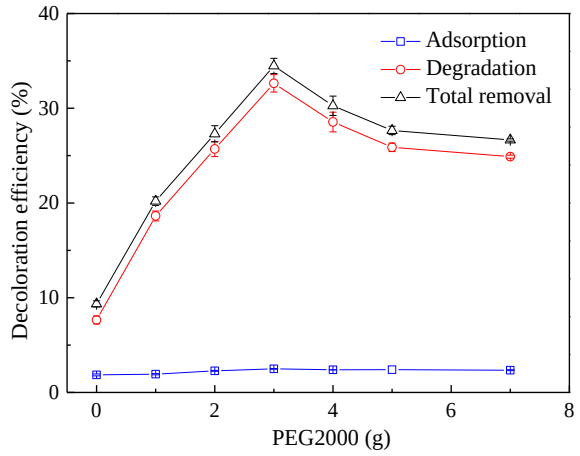

Fig. 5. Adsorption and photocatalytic degradation of azophloxine on $La_2Ti_2O_7$ as a factor of PEG2000 amount

Fig. 6 shows UV-Vis spectra of azophloxine solution during photocatalytic degradation with respect to PEG2000 amount. The broad absorption band between 400 and 600 nm is due to the azo conjugated system of azophloxine. The maximum absorption intensity of this chromophore group situates at 506 nm, which can be used to determine the concentration of this azo dye. The intrinsic absorption of benzene ring and naphthalene ring is at 235 nm, while the absorption at 320 nm is due to the interplay of benzene ring and naphthalene ring with the chromophore group. The weak absorption peak at 249 nm is related to n-π conjugated absorption of secondary amide.

The absorption intensities of the above-mentioned peaks are reduced during photocatalytic degradation, indicating the decomposition of these functional groups in azophloxine molecule. The intensity reducing rate is in accordance to the activity of the materials. As can be seen in Fig. 6c, nearly all the absorptions disappear after 180 min of reaction in the solution containing the $La_2Ti_2O_7$ sample obtained with 3 g PEG2000. In order to make kinetic determination of photocatalytic degradation of azophloxine, the first order reaction rate was calculated to compare the materials. The reaction rate constant is 0.0032 min^{-1} for the $La_2Ti_2O_7$ sample prepared without PEG2000, while the reaction rate constants are promoted to 0.0135 and 0.0191 min^{-1} when 1 and 3 g of PEG2000 were used to prepare the porous $La_2Ti_2O_7$ sample.

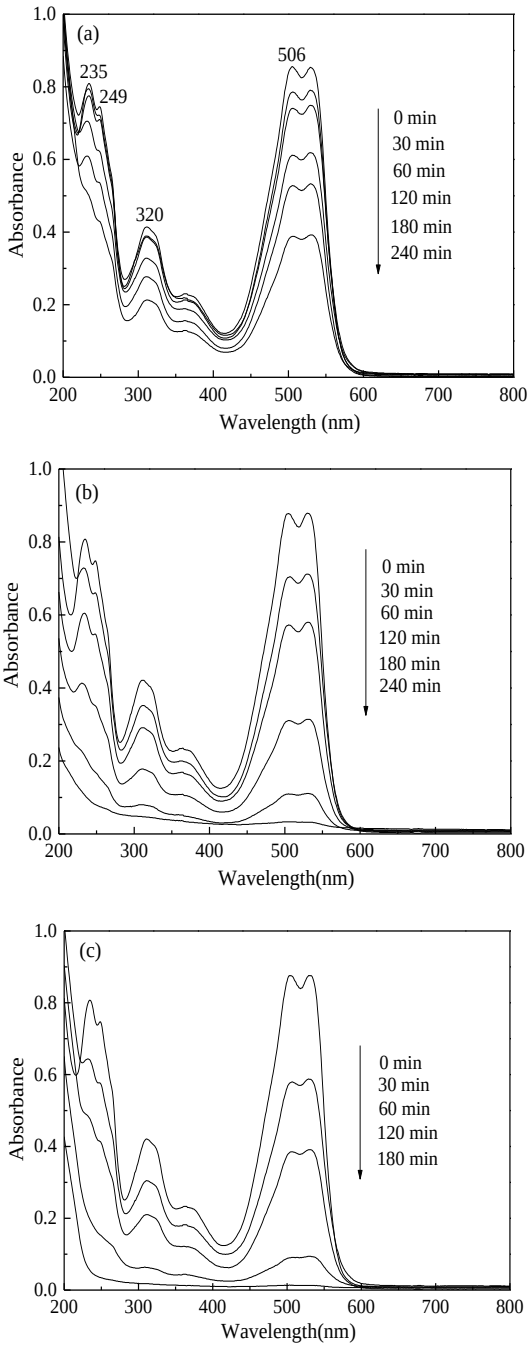

Fig. 6. UV-Vis spectra of azophloxine solution during photocatalytic degradation with respect to PEG2000 amount. (a) 0 g, (b) 1 g, (c) 3 g

4. Conclusions

The effects of PEG2000 on the properties of lanthanum titanate materials were examined in this work. The existence of PEG2000 in the precursor retards the crystal growth of perovskite $La_2Ti_2O_7$. Both BET surface area and total pore volume of the samples are enlarged after using PEG2000. The absorption intensities of the bondings in $La_2Ti_2O_7$ decrease after using more PEG2000. The degradation efficiency is increased almost linearly with rising PEG2000 amount and reaches the maximum value when 3 g of PEG2000 was used to prepare the porous $La_2Ti_2O_7$ sample. Decomposition of the functional groups in azophloxine molecule is identified.

Acknowledgments

This work was supported by National Natural Science Foundation for Youths of China (No. 51504154), Research on Basic Science and Technology in Universities Supported by Education Department of Liaoning Province (LG201706), and Scientific Research Project of Liaoning Provincial Education Department (No. LG201913).

References

[1] M. R. Hoffmann, S. T. Martin, W. Choi, W. Bahnemann, Chem. Rev. **95**, 69 (1995).
[2] A. Fujishima, T. N. Rao, D. A. Tryk, J. Photochem. Photobio. C **1**, 1 (2000).
[3] W. J. Zhang, J. Yang, C. G. Li, Mater. Sci. Semicond. Process. **85**, 33 (2018).
[4] Z. Zhu, P. Huo, Z. Lu, Y. Yan, Z. Liu, W. Shi, C. Li, H. Dong, Chem. Eng. J. **331**, 615 (2018).
[5] W. Zhang, F. Bi, Y. Yu, H. He, J. Mole. Catal. A: Chem. **372**, 6 (2013).
[6] Z. Li, M. Qi, C. Tu, W. Wang, J. Chen, A. J. Wang, Appl. Surf. Sci. **425**, 765 (2017).
[7] G. Gupta, A. Umar, A. Kaur, S. Sood, A. Dhir, S. K. Kansal, Mater. Res. Bull. **99**, 359 (2018).
[8] G. Sharma, S. Bhogal, M. Naushad, A. Kumar, F. J. Stadler, J. Photoch. Photobio. A: Chem. **347**, 235 (2017).
[9] W. J. Zhang, Y. J. Tao, C. G. Li, Mater. Res. Bull. **105**, 55 (2018).
[10] W. Zhang, Y. Liu, X. Pei, X. Chen, J. Phys. Chem. Solids **104**, 45 (2017).
[11] W. Zhang, L. Du, F. Bi, H. He, Mater. Lett. **157**, 103 (2015).
[12] J. Chen, S. Liu, L. Zhang, N. Chen, Mater. Lett. **150**, 44 (2015).
[13] W. J. Zhang, H. L. Li, Z. Ma, H. Li, H. Wang, Solid State Sci. **87**, 58 (2019).
[14] Z. Chen, H. Jiang, W. Jin, C. Shi, Appl. Catal. B: Environ. **180**, 698 (2016).
[15] W. Zhang, Y. Tao, C. Li, Solid State Sci. **78**, 16 (2018).
[16] L. M. Lozano-Sánchez, S. Obregón, L. A. Díaz-Torres, S. Lee, V. Rodríguez-González, J. Mol. Catal. A: Chem. **410**, 19 (2015).
[17] Y. A. Zulueta, M. T. Nguyen, J. Phys. Chem. Solids **121**, 151 (2018).
[18] B. Kiss, T. D. Manning, D. Hesp, C. Didier, M. J. Rosseinsky, Appl. Catal. B: Environ. **206**, 547 (2017).
[19] K. Katagiri, Y. Miyoshi, K. Inumaru, J. Colloid Interface Sci. **407**, 282 (2013).
[20] Z. L. Hua, X. Y. Zhang, X. Bai, L. L. Lv, Z. F. Ye, X. Huang, J. Colloid Interface Sci. **450**, 45 (2015).
[21] W. J. Zhang, Z. Ma, L. Du, L. L. Yang, X. J. Chen, H. B. He, J. Alloys Compds. **695**, 3541 (2017).
[22] H. Chang, E. Jo, H. Jang, T. Kim, Mater. Lett. **92**, 202 (2013).
[23] S. Brunauer, P. H. Emmett, E. Teller, J. Am. Chem. Soc. **60**, 309 (1938).
[24] E. P. Barrett, L. G. Joyner, P. P. Halenda, J. Am. Chem. Soc. **73**, 373 (1951).
[25] W. J. Zhang, Y. X. Liu, C. G. Li, J. Phys. Chem. Solids **118**, 144 (2018).
[26] A. Patterson, Phys. Rev. **56**, 978 (1939).
[27] K. Onozuka, Y. Kawakami, H. Imai, T. Yokoi, T. Tatsumi, J.N. Kondo, J. Solid State Chem. **192**, 87 (2012).
[28] J. Lian, J. He, X. Zhang, Solid State Sci. **61**, 9 (2016).

*Corresponding author: wjzhang@aliyun.com